Available online at www.sciencedirect.com

ScienceDirect

Geochimica et Cosmochimica Acta 139 (2014) 313–326

Geochimica et Cosmochimica Acta

www.elsevier.com/locate/gca

Diffusion of multi-isotopic chemical species in molten silicates

James M. Watkins [a,*], Yan Liang [b], Frank Richter [c], Frederick J. Ryerson [d], Donald J. DePaolo [e]

[a] Dept. of Geological Sciences, University of Oregon, United States
[b] Dept. of Geological Sciences, Brown University, United States
[c] Dept. of Geophysical Sciences, University of Chicago, United States
[d] Lawrence Livermore National Laboratory, United States
[e] Earth Sciences Division, Lawrence Berkeley National Laboratory, United States

Received 19 September 2013; accepted in revised form 23 April 2014; Available online 9 May 2014

Abstract

Diffusion experiments in a simplified Na_2O–CaO–SiO_2 liquid system are used to develop a general formulation for the fractionation of Ca isotopes during liquid-phase diffusion. Although chemical diffusion is a well-studied process, the mathematical description of the effects of diffusion on the separate isotopes of a chemical element is surprisingly underdeveloped and uncertain. Kinetic theory predicts a mass dependence on isotopic mobility, but it is unknown how this translates into a mass dependence on effective binary diffusion coefficients, or more generally, the chemical diffusion coefficients that are housed in a multicomponent diffusion matrix. Our experiments are designed to measure Ca mobility, effective binary diffusion coefficients, the multicomponent diffusion matrix, and the effects of chemical diffusion on Ca isotopes in a liquid of single composition.

We carried out two chemical diffusion experiments and one self-diffusion experiment, all at 1250 °C and 0.7 GPa and using a bulk composition for which other information is available from the literature. The self-diffusion experiment is used to determine the mobility of Ca in the absence of diffusive fluxes of other liquid components. The chemical diffusion experiments are designed to determine the effect on Ca isotope fractionation of changing the counter-diffusing component from fast-diffusing Na_2O to slow-diffusing SiO_2. When Na_2O is the main counter-diffusing species, CaO diffusion is fast and larger Ca isotopic effects are generated. When SiO_2 is the main counter-diffusing species, CaO diffusion is slow and smaller Ca isotopic effects are observed. In both experiments, the liquid is initially isotopically homogeneous, and during the experiment Ca isotopes become fractionated by diffusion. The results are used as a test of a new general expression for the diffusion of isotopes in a multicomponent liquid system that accounts for both self diffusion and the effects of counter-diffusing species.

Our results show that (1) diffusive isotopic fractionations depend on the direction of diffusion in composition space, (2) diffusive isotopic fractionations scale with effective binary diffusion coefficient, as previously noted by Watkins et al. (2011), (3) self-diffusion is not decoupled from chemical diffusion, (4) self diffusion can be faster than or slower than chemical diffusion and (5) off-diagonal terms in the chemical diffusion matrix have isotopic mass-dependence. The results imply that relatively large isotopic fractionations can be generated by multicomponent diffusion even in the absence of large concentration gradients of the diffusing element. The new formulations for isotope diffusion can be tested with further experimentation and provide an improved framework for interpreting mass-dependent isotopic variations in natural liquids.

* Corresponding author. Tel.: +1 5102255043.
E-mail address: watkins4@uoregon.edu (J.M. Watkins).

http://dx.doi.org/10.1016/j.gca.2014.04.039
0016-7037/

1. INTRODUCTION

The trace element and isotopic composition of mineral phases can be used to probe the temperatures and rates of mineral formation as well as the degree of post-mineralization alteration. The accuracy with which these effects can be interpreted is limited by our knowledge of three key parameters and their relative importance in determining the composition of a mineral grain and its surroundings: (1) thermodynamic (equilibrium) partitioning, (2) diffusion coefficients, and (3) reaction rate constants. The latter two are typically lumped together as "kinetic" parameters even though they are distinct. Understanding the mechanisms of diffusion and reaction in geological liquids, and how these mass transport processes discriminate between isotopes, represents an important problem for interpreting the isotopic composition of geologic materials (Richter et al., 1999, 2003, 2009; Roskosz et al., 2006; Watkins et al., 2009, 2011; Goel et al., 2012), as well as a fundamental materials science problem that relates to the structure and dynamics of complex liquids.

Our focus in this work is on mass transport by chemical diffusion in silicate liquids. Liquid phase diffusion is inherently complex, and we show in this work that the effects of liquid phase diffusion on isotopic species poses additional challenges. Diffusion experiments on silicate liquids have documented that isotopic species diffuse at different rates depending on mass, which can result in large transient variations in isotopic ratios (cf. Watkins et al. (2011) for a summary). In the relatively simple case of trace element diffusion, the tracer diffuses in response to its own concentration gradient. Since the concentration of a tracer is low by definition, counter gradients in other components and associated changes in melt structure, are negligible. As the concentration of the diffusing component increases to the point where the diffusing species constitutes a substantial fraction of the mass or volume of the bulk material, the melt components that compose the melt structure must also diffuse to balance the net flux of the diffusing component (Liang et al., 1996). In systems with large concentration gradients in multiple major components, diffusive coupling arises through thermodynamic activity-composition relations and kinetic interactions among different diffusing species or components (e.g., differences in mobility, size, and charge). In most natural systems, diffusion of all major components can be treated using a matrix of diffusion coefficients where the off-diagonal terms describe diffusive coupling (Onsager, 1945; de Groot and Mazur, 1963).

The full diffusion matrix has only been determined for a few simplified silicate liquid compositions (e.g., Sugawara et al., 1977; Kress and Ghiorso, 1993; Trial and Spera, 1994; Chakraborty et al., 1995; Liang et al., 1996; Richter et al., 1998; Liang, 2010), but no study has yet determined the diffusion matrix for the element fluxes and the mass dependence on the isotope fluxes simultaneously. There is evidence from diffusion experiments involving natural silicate liquids that coupling between components affects the sign and magnitude of isotope fractionation, but these effects are not yet well understood (Watkins et al., 2009). In this study we measure both the diffusion matrix and isotopic fractionation by diffusion along different directions in composition space for the relatively simple $CaO–Na_2O–SiO_2$ (CNS) system. Because this system is Al_2O_3-free, Na_2O and CaO should exist exclusively as network-modifying components, avoiding complications associated with their role in charge-compensating tetrahedrally coordinated Al. This makes the system relatively "simple," but nevertheless there are still substantial complexities, and the exclusion of Al eliminates other effects that are critical for real silicate systems and have been shown to be important for understanding isotopic fractionation for elements like Ca that tend to be closely coupled to Al (Watkins et al., 2009).

2. THEORY FOR MULTICOMPONENT CHEMICAL AND SELF DIFFUSION

In this section we endeavor to lay out the equations and considerations that are necessary to describe the diffusion of a multi-isotopic chemical species in a silicate liquid. Along the way we provide a reminder of various definitions, assumptions, and requirements, and hope that this exposition will make the later discussion comprehensible. Some of this material can be found elsewhere, but the review here is necessary because we ultimately need equations that describe isotopic effects during diffusion and also conserve mass, equations that have not been presented in any previous work.

2.1. A general expression for the diffusive flux

In the absence of chemical sinks, sources, and advection, the change in concentration of component i in a fluid volume element is given by (de Groot and Mazur, 1963):

$$\frac{\partial C_i}{\partial t} = -\nabla \cdot J_i, \tag{1}$$

where C is molar concentration (moles/m^3), ∇ is the gradient operator, and J is molar flux (moles/m^2/s). In a volume-fixed frame of reference, the diffusive flux of isotope k of element i can be written as:

$$J_i^k = \underbrace{-D_i^k \nabla C_i^k + \sum_{m=1}^{M} f_i^k D_i^m \nabla C_i^m}_{\text{self diffusion}} \underbrace{- \sum_{j=1}^{n-1} f_i^k D_{ij}^k \nabla C_j}_{\text{chemical diffusion}}, \tag{2}$$

where D_i^k is the self diffusion coefficient of isotope k; C_i^k is the molar concentration of isotope k; M is the number of isotopes for element i; f_i^k is the mole fraction of k in element i; C_j is the molar concentration of element j; and the D_{ij}^k's are elements of the multicomponent diffusion matrix (Liang, 2010). The sum on the RHS is taken over $n-1$ components because only $n-1$ independent fluxes are required to describe the system. The nth component is referred to as the dependent component. Eq. (2) differs slightly from the equation for the isotopic flux used in previous studies (e.g., Richter et al., 1999, 2003; Watkins et al., 2011) for reasons that are described in Appendix A.1.

Eq. (2) is self-consistent for the two limiting cases: (a) multicomponent diffusion and (b) self diffusion. In the case of multicomponent diffusion, if we sum Eq. (2) for all the isotopes of component i, we have

$$\sum_{k=1}^{M} J_i^k = -\sum_{k=1}^{M} D_i^k \nabla C_i^k + \sum_{k=1}^{M}\left(\sum_{m=1}^{M} f_i^k D_i^m \nabla C_i^m\right) - \sum_{k=1}^{M}\left(\sum_{j=1}^{n-1} f_i^k D_{ij}^k \nabla C_j\right). \quad (3)$$

Since $\sum_{k=1}^{M} f_i^k = 1$, we have the standard expression for the diffusive flux in a multicomponent fluid (de Groot and Mazur, 1963),

$$J_i = \sum_{k=1}^{M} J_i^k = -\sum_{j=1}^{n-1} D_{ij}^k \nabla C_j. \quad (4)$$

In the case of self diffusion, the bulk concentration gradients are zero and Eq. (2) takes the form

$$J_i^k = -D_i^k \nabla C_i^k + \sum_{m=1}^{M} f_i^k D_i^m \nabla C_i^m. \quad (5)$$

Since $C_i = C_i^1 + C_i^2 + \ldots + C_i^M = \text{constant}$ in the case of self diffusion, we have $\nabla C_i^M = -\sum_{m=1}^{M-1} \nabla C_i^m$, and Eq. (5) can then be written as

$$J_i^k = -D_i^k \nabla C_i^k - \sum_{m=1}^{M-1} f_i^k (D_i^M - D_i^m) \nabla C_i^m. \quad (6)$$

Eq. (6) is a more generalized expression for self diffusion in a fluid system in which bulk concentration gradients are absent and mobilities of individual isotopes are slightly different from each other. When self diffusivities are the same among the isotopes for a given element, Eq. (6) recovers the standard expression for self diffusion , i.e., $J_i^k = -D_i^k \nabla C_i^k$. Eq. (6) is identical, in form, to the molecular common velocity model derived by Liang (1994) where the isotopes are treated as components in the special case of self diffusion.

2.2. Effective binary diffusion of an isotope

For many applications the diffusion matrix is not known, and it is common practice to determine effective binary diffusion coefficients (EBDCs) of major elements using an effective binary diffusion (EBD) model (e.g., Cooper, 1968). When only EBDCs are available, which is the case for chemical diffusion in natural silicates, the diffusive flux of isotope k of element i may be written as

$$J_i^k = -D_i^k \nabla C_i^k - f_i^k (D_i^E - D_i^k) \nabla C_i - \sum_{m=1}^{M} f_i^k (D_i^m - D_i^k) \nabla C_i^m, \quad (7a)$$

where

$$D_i^E = \sum_{j=1}^{n-1} D_{ij}^k \frac{\partial C_j}{\partial C_i}. \quad (7b)$$

In Eqs. (7a) and (7b), D_i^E is the EBDC of component i in the melt while holding all other components as the dependent variable (Cooper, 1968). Since EBDCs depend on concentration gradients of all other components, they are highly sensitive to the bulk composition of the system, the orientation of a given diffusion couple in composition space, the diffusion geometry, and the diffusion time (Liang, 2010). The utility of EBD models is that a single parameter can describe the flux of an oxide component for a specific situation, but EBDCs are not generalizable to other situations even within the same compositional system (Liang et al., 1996). The main advantage of the diffusion matrix representation of chemical fluxes is that only one set of $n-1 \times n-1$ diffusion parameters is needed to accurately describe the chemical fluxes for all components and directions of diffusion in composition space. *It is unclear, however, whether an analogous general expression exists for diffusion of isotopes, i.e., whether a single set of isotope-specific diffusion coefficients can accurately describe the isotopic fluxes for all directions of diffusion in composition space.*

2.3. Isotope fractionation by diffusion

During chemical diffusion, the isotopes of an element can become fractionated owing to the greater mobility of lighter isotopes over heavier isotopes. The greater net flux of lighter isotopes can be due to a greater average velocity (because of same average kinetic energy) or shorter average lifetime of chemical bonds. Regardless of the specific mechanism(s) of diffusion, the mass dependence of isotopic self diffusion coefficients can be described by a semi-empirical power law relationship (Richter et al., 1999):

$$\frac{D_i^H}{D_i^L} = \left(\frac{m_L}{m_H}\right)^{\beta_i}, \quad (8a)$$

where m is the mass of the isotope (not the isotope-specific oxide), and the letters L and H refer to the light isotope and heavy isotope, respectively. The β_i parameter describes the efficiency of isotope fractionation by diffusion. Larger β_i corresponds to a greater difference between isotopic diffusion coefficients; in gases β_i can approach 0.5 but in silicate liquids it is observed to be in the range 0.020–0.215 (Watkins et al., 2011). We note that m is the mass of the cation, and does not account for the cation's affinity for different molecular species within the melt. In this respect, the influence of cation speciation is manifest in beta and is expected to vary with melt composition (Watkins et al., 2009).

The mass dependence on self diffusivity, or mobility, should also be manifest in a mass dependence on chemical diffusion coefficients, but there is not yet a function that relates isotopic self diffusion coefficients to isotope-specific chemical diffusion coefficients. For now we define additional β's related to elements of the diffusion matrix:

$$\frac{D_{ij}^H}{D_{ij}^L} = \left(\frac{m_L}{m_H}\right)^{\beta_{ij}}, \quad (8b)$$

and a β related to effective binary diffusion

$$\frac{D_i^{E,H}}{D_i^{E,L}} = \left(\frac{m_L}{m_H}\right)^{\beta_i^E}. \quad (8c)$$

A test of whether the individual elements of the multicomponent diffusion matrix are mass dependent requires knowledge of the diffusion matrix and measurable diffusive isotopic fractionations. These two factors guide our experimental approach.

3. EXPERIMENTAL METHODS

3.1. Diffusion couple experiments

The simplest case – a ternary system with a 2 × 2 diffusivity matrix – requires two diffusion couples (Trial and Spera, 1994). Here we have chosen to investigate diffusion in the $16Na_2O{\cdot}12CaO{\cdot}72SiO_2$ (wt%) system using the same starting compositions as Wakabayashi and Oishi (1978) (Fig. 1) for two reasons. First, the run conditions for their experiments are known, and are easily accessible employing the standard 19-mm piston-cylinder assembly used in our laboratory. Second, their diffusion couples represent a case where the EBDC for CaO varies substantially depending on the orientation of the diffusion couples in composition space. In the two experiments we present, CaO diffuses down a substantial concentration gradient. In couple A–B, there is a significant Na_2O gradient but only a small initial SiO_2 gradient. In couple D–E, there is a significant SiO_2 gradient, but only a small Na_2O gradient. In both cases the initial Ca isotope composition is uniform and our assessment of diffusive isotope effects comes from the isotopic variations that develop during the experiment.

Compositions labeled A, B, D, E and S (Fig. 1 and Table 1) were synthesized from reagent-grade oxides and carbonates. These sample labels are consistent with those used in Wakabayashi and Oishi (1978). The mixtures were ground together under ethanol in a Retsch automated mortar and pestle. For the self diffusion experiment, 1 g of composition S was spiked with 0.0046 g of ^{44}Ca (Oak Ridge National Laboratory Batch no. 192701). All mixtures were calcined overnight in a platinum crucible at 850 °C and then fused at 1450 °C under atmospheric conditions in a Deltech furnace. After about 45 min, the melt was quenched to glass and remixed in the automated mortar and pestle. The mixture was dried under a heat lamp and stored in an oven at 110 °C.

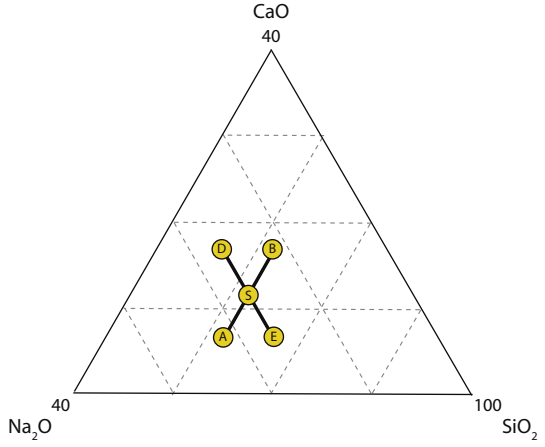

Fig. 1. Starting compositions in wt% for diffusion couples in the $CaO–Na_2O–SiO_2$ ternary. Couples A–B and D–E are the same compositions and labels used by Wakabayashi and Oishi (1978). Composition S is the bulk composition of the system as well as the approximate bulk composition for both halves of the self diffusion experiment.

Table 1
Nominal starting compositions in wt% for diffusion couples in the $CaO–Na_2O–SiO_2$ system.

	A	B	D	E	S
CaO	7	17	17	7	12
Na_2O	21	11	16	16	16
SiO_2	72	72	67	77	72
Total	100	100	100	100	100

Table 2
Ca isotope compositions measured on post-run diffusion couples. The isotopic compositions represent an average for each wafer. A conservative estimate for error bars on $\Delta^{44}Ca$ is ±0.15‰.

Sample	Distance (mm)	$\Delta^{44}Ca$ (‰)	Number of analyses
AB-1	−2.80	−0.59	2
AB-2	−2.17	−0.88	2
AB-3	−1.53	−1.31	2
AB-4	−0.90	−1.46	2
AB-5	−0.26	−0.28	2
AB-6	0.38	0.64	2
AB-7	1.01	0.72	3
AB-8	1.65	0.00	2
AB-9	2.28	−0.07	2
AB-10	2.92	0.10	3
DE-1	−2.25	0.00	2
DE-2	−1.62	−0.32	2
DE-3	−0.98	−0.57	2
DE-4	−0.35	−0.89	2
DE-5	0.29	0.10	2
DE-6	0.93	0.28	2
DE-7	1.56	0.06	2
DE-8	2.20	0.02	2
DE-9	2.83	−0.03	2
DE-10	3.47	0.18	3

Each diffusion couple experiment was assembled by juxtaposing two powders of different composition atop one another in a graphite capsule (I.D. = 3.4 mm). The capsule was placed in a standard $\frac{3}{4}$-inch piston cylinder assembly and cold-pressurized to about 8 kbar. The sample was brought to 1250 °C at a ramp rate of 100 °C/min and held at run conditions for 1 h. The total variation in temperature across the experimental capsule was estimated to be less than 20 °C based on isotopic variations produced in a basalt-only experimental run at 1450 °C (Watkins et al., 2009). The pressure was not adjusted during the ramp or run.

3.2. Electron microprobe analyses

Post-run diffusion couples are sectioned down their vertical axis and axis-parallel major-element profiles are measured with a JEOL JXA-8200 SuperProbe at Lawrence Livermore National Laboratory. We use a 15 nA beam current rastered at 12,000× magnification (12 μm × 9 μm beam dimensions) with an accelerating voltage of 15 kV. Sodium is measured first at each spot to mitigate effects of Na migration. For the purpose of fitting the measured profiles, the oxide concentrations are normalized to 100 wt% and any impurities including water are ignored.

3.3. Ca isotope analyses

For the self diffusion experiment, $^{44}Ca/^{40}Ca$ ratios were measured at Lawrence Livermore National Laboratory using a modified Cameca ims-3f ion microprobe. The sample was sputtered using a static ^{16}O primary ion beam at 12.5 keV with beam currents ranging between 0.2 to 0.3 nA, producing spot sizes of about 10 μm in diameter. Positive secondary ions of ^{28}Si, ^{40}Ca, ^{42}Ca, ^{43}Ca, and ^{44}Ca were accelerated at 4500 V and mass analyzed at a mass resolving power ($m/\Delta m$) high enough (>2000) to separate potential interfering species of $^{24}Mg^{16}O^+$ and $^{28}Si^{16}O^+$ from the atomic ^{40}Ca and ^{44}Ca ions respectively. To avoid crater-edge effects a field aperture was inserted in the sample image plane, effectively allowing only secondary ions from a 30 μm diameter region of the sample surface. A typical analysis consisted of 40 individual mass scans with count times of 1 s for each mass and count rates high enough (>4000 cps on mass 44) to make the background (0.01 cps) correction insignificant.

For all other isotope analyses, diffusion couples were sectioned into wafers, about 465 μm thick and weighing about 3 mg, using a Bico diamond wafer saw with blade thickness of 165 μm. The wafers were dissolved in a mixture of 8–12 drops hydrofluoric acid and 2 drops perchloric acid. Samples were treated in the following steps: (1) dried at 165 °C, (2) redissolved in 5 mL 3N HNO_3, (3) aliquotted, (4) spiked, (5) dried, and (6) redissolved in 100 μL 3N HNO_3. Next, the Ca fraction was separated and collected by cation exchange chromatography using Eichrom Ca-spec DGA resin. Ca isotope ratio measurements were carried out by thermal ionization mass spectrometry (TIMS) at UC-Berkeley on a Thermo-Finnigan Triton TI with nine moveable Faraday collectors. The Ca isotope composition is expressed as:

$$\delta^{(44/40)}Ca_{sample} = \delta^{44}Ca_{sample} = 1000 \cdot \left[\frac{\left(^{44}Ca/^{40}Ca\right)_{sample}}{0.0212076} - 1 \right]. \quad (9)$$

The magnitude of diffusive isotopic fractionations is given by

$$\Delta^{44}Ca = \delta^{44}Ca_{sample} - \delta^{44}Ca_{initial}, \quad (10)$$

where 'initial' denotes the isotopic composition of the starting material. Calcium isotope compositions are provided in Table 2.

4. EXPERIMENTAL RESULTS

4.1. Self diffusion experiment

Fig. 2 shows results of our self diffusion experiment in which there is a large gradient in the minor isotope ^{44}Ca but negligible gradient in CaO. For the unspiked side of the capsule, the approximate abundances of ^{44}Ca and ^{40}Ca are 2% and 96% of total Ca, respectively. The measured $^{44}Ca/^{40}Ca$ profile is symmetric about the interface, as expected for diffusion of a tracer in a compositionally homogeneous liquid.

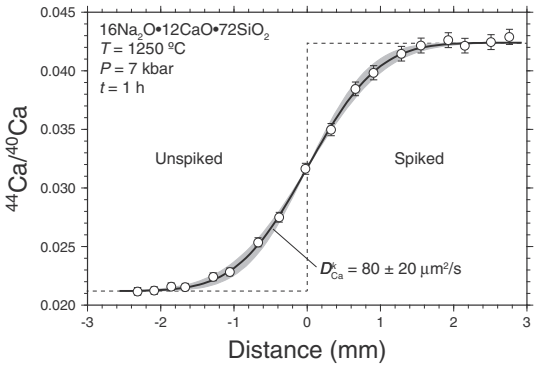

Fig. 2. Self diffusion of Ca in the $16Na_2O{\cdot}12CaO{\cdot}72SiO_2$ system. The bulk composition is initially uniform on both sides of the capsule, but the $^{44}Ca/^{40}Ca$ ratio differs by a factor of 2. In the absence of chemical gradients, the rate of isotopic homogenization is given by the self diffusivity.

4.2. Major element profiles

The measured diffusion profiles cast in terms of wt% oxide components are shown in Fig. 3. The key feature to note is the difference in diffusion behavior of CaO between A–B and D–E. In experiment A–B, the CaO profile is clearly more evolved than in experiment D–E despite the fact that both couples were run for 1 h and share the same bulk composition. In experiment A–B, the flat SiO_2 gradient is accompanied by a monotonic gradient in Na_2O, while in experiment D–E, the steep gradient in SiO_2 is accompanied by uphill diffusion of Na_2O. These observations are in agreement with previous experiments that used the same starting compositions but slightly different run conditions (1200 °C and 1 atm; Wakabayashi and Oishi, 1978).

4.3. Ca isotope profiles

The bottom panels of Fig. 3 show the measured Ca isotopic fractionations (Fig. 3d and h). In both experiments, the simple diffusion gradients indicate that the net flux of CaO is in the direction of its own concentration gradient, and since diffusivity is inversely related to mass, the lighter isotope ^{40}Ca diffuses faster and is enriched (lower $^{44}Ca/^{40}Ca$) in the CaO-poor side of the diffusion couple. In couple A–B, which experienced faster diffusion of CaO, the magnitude of isotopic fractionations is larger (2.5‰) than in couple D–E (1.3‰). In these types of experiments the magnitude of isotopic fractionations is not expected to vary with duration of the experiment until the *minimum* in $\Delta^{44}Ca$ reaches the end of the capsule. The profiles for A–B and D–E thus represent the first experimental evidence that the magnitude of diffusive isotope effects varies with the direction of diffusion in composition space. It is also important to note that there is no obvious evidence of isotopic fractionation due to undesired temperature gradients in either experiment, suggesting either there is a negligible temperature gradient in our experimental capsule or Ca isotopes are not sensitive to temperature gradients in this ternary silicate liquid system.

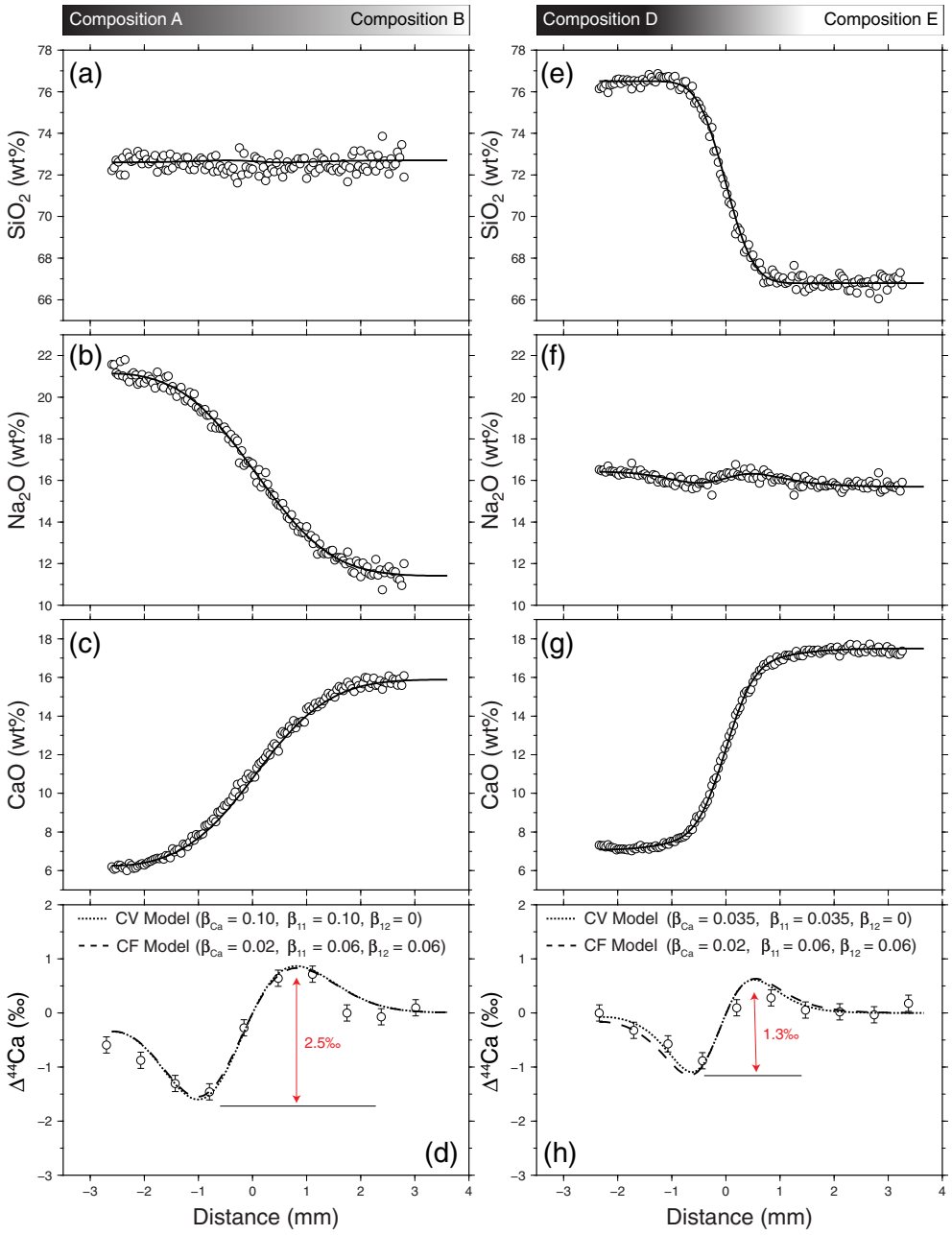

Fig. 3. Chemical diffusion profiles in the system $16Na_2O{\cdot}12CaO{\cdot}72SiO_2$. Panels (a)–(c): Diffusion couple A–B has little to no initial SiO_2 gradient and both CaO and Na_2O diffuse relatively fast. Panels (e)–(g): Diffusion couple D–E has little to no initial Na_2O gradient and both CaO and SiO_2 diffuse relatively slow. Solid lines are model concentration profiles using the matrix representation of diffusive fluxes (see text and Eq. 12). Panels (d) and (h): Calcium isotope fractionations due to multicomponent chemical diffusion. Solid lines are model isotope profiles produced using the diffusion matrix representation with a mass dependence on diffusivity parameters (see text and Eqs. (16a) and (16b)). Estimated confidence interval on the β parameters is about ± 0.01.

5. MODELING RESULTS

The following discussion is aimed at reconciling the effects of pure "self diffusion," in which isotopes of a certain element redistribute themselves in a situation where there is no gradient in the chemical concentration of the element, and "chemical diffusion," where there is no initial difference in isotopic composition but a large concentration gradient. In the latter, although there are no isotopic gradients at the beginning of an experiment, isotopic gradients develop during the experiment, and thereafter both "chemical diffusion" and "self diffusion" are operating to produce isotopic gradients. These effects were discussed by Watkins et al. (2011) but in the context of an incomplete theoretical treatment (Appendix A.1).

5.1. Self diffusion

The self diffusivity of Ca at composition 'S,' , based on the data shown in Fig. 2, is determined by combining Eqs. (1) and (6) and simultaneously solving for the time evolution of ^{44}Ca and ^{40}Ca concentration profiles:

$$\frac{\partial C_i^k}{\partial t} = D_i^k \nabla^2 C_i^k - \nabla \cdot \sum_{m=1}^{M-1} f_i^k (D_i^M - D_i^m) \nabla C_i^m. \tag{11}$$

For this problem, where there is initially a large gradient in the isotopic ratio, the inferred self diffusivity is insensitive to differences in isotopic diffusion coefficients. The best-fit ^{44}Ca/^{40}Ca profile in Fig. 2 corresponds to $D_{\mathrm{Ca}}^k = 80 \pm 20$ μm^2/s, which represents a weighted average of Ca isotopic self diffusivities.

5.2. Multicomponent chemical diffusion and [D] values

Major-element diffusion profiles are modeled by solving a system of equations based on Eqs. (1) and (4) and assuming the D_{ij}'s are constant as a function of composition:

$$\frac{\partial C_i}{\partial t} = \sum_{j=1}^{n-1} D_{ij} \nabla^2 C_j. \tag{12}$$

Since the diffusion couples are not long enough to be regarded as infinite for these experiments, we use the no-flux boundary condition at either end of the domain:

$$\nabla C_i = 0 \quad \text{at} \quad x = \text{LHS} \quad \text{and} \quad x = \text{RHS}, \tag{13}$$

where LHS and RHS refer to the left-hand side and right-hand side of the capsule, which are not symmetric about the initial interface. Note that, in using Eq. (12), we are implicitly ignoring the isotopic variability of diffusion coefficients, and treating each element as if it had only one isotope, or alternatively, as if the concentration profile can be described by a single, average diffusion coefficient. For Ca, because ^{40}Ca constitutes roughly 97% of all calcium isotopes, the diffusion coefficient for bulk calcium is effectively indistinguishable from the diffusion coefficient for ^{44}Ca.

The elements of the 2 × 2 diffusion matrix are obtained by the full nonlinear joint inversion method (Liang, 1994; Liang, 2010). The best-fit [**D**] matrix with SiO_2 as the dependent component is (± values represent 95% confidence intervals):

$$[\mathbf{D}] = \begin{bmatrix} D_{\mathrm{CaO-CaO}} & D_{\mathrm{CaO-Na_2O}} \\ D_{\mathrm{Na_2O-CaO}} & D_{\mathrm{Na_2O-Na_2O}} \end{bmatrix} = \begin{bmatrix} 47 \pm 3 & -116 \pm 7 \\ -25 \pm 4 & 144 \pm 7 \end{bmatrix} \cdot 10^{-12}\ \mathrm{m^2/s}, \tag{14}$$

or with Na_2O as the dependent component:

$$[\mathbf{D}] = \begin{bmatrix} D_{\mathrm{CaO-CaO}} & D_{\mathrm{CaO-SiO_2}} \\ D_{\mathrm{SiO_2-CaO}} & D_{\mathrm{SiO_2-SiO_2}} \end{bmatrix} = \begin{bmatrix} 163 \pm 6 & 116 \pm 7 \\ 6 \pm 4 & 28 \pm 4 \end{bmatrix} \cdot 10^{-12}\ \mathrm{m^2/s}. \tag{15}$$

The above [**D**] values are defined with concentrations expressed in weight percent oxide components. If concentrations were expressed using different components or different units such as mole fraction, the values of the elements of the diffusion matrix would be slightly different but the conclusions we draw in this study would be the same. When components j and i are counter diffusing; i.e., their gradients are opposite in sign, a negative D_{ij} indicates that component j enhances the diffusive flux of i. Conversely, a positive D_{ij} indicates that component j suppresses the diffusive flux of i. In this system, the large negative value of $D_{\mathrm{CaO-Na_2O}}$ corresponds to the enhancement of the Ca diffusive flux due to counter-diffusing Na, while the large positive value of $D_{\mathrm{CaO-SiO_2}}$ is indicative of the suppression of the Ca diffusive flux due to counter diffusing Si. The excellent agreement between model and measured profiles (Fig. 3) provides support for the assumption of constant D_{ij}^k values over the (relatively narrow) range of compositions spanned by each diffusion couple.

5.3. Isotope diffusion and β factors

There is no generally accepted approach for how to model isotope fractionation by multicomponent chemical diffusion, and mass dependent isotope fractionation by diffusion has not been modeled for a system in which the full diffusion matrix is known. Richter et al. (2003) established the groundwork by employing an effective binary diffusion model where each isotope was treated as an independent chemical species, diffusing in response to its own concentration gradient. As discussed earlier, however, the diffusion parameters D_i^{E} and β_i^{E} obtained by EBD models are non-generalizable and specific to a given direction of diffusion in composition space. In contrast, the multicomponent diffusion equation can reproduce the major element profiles in both experiments with a single set of diffusion matrix elements.

For the diffusive isotope fractionation problem, it is important to include all terms of Eq. (2), describing both chemical and self diffusion. For simplicity we use only two of the six stable isotopes of Ca, ^{44}Ca and ^{40}Ca, but note that inclusion of additional isotopes does not affect the model ^{44}Ca/^{40}Ca profiles. Model isotopic concentration profiles are calculated from the following system of equations based on Eq. (2) with SiO_2 as the dependent component (1 = CaO and 2 = Na_2O):

$$\begin{aligned} \frac{\partial C_1^{40}}{\partial t} = {} & D_1^{40} \nabla^2 C_1^{40} - \nabla f_1^{40} D_1^{40} \nabla C_1^{40} - f_1^{40} D_1^{40} \nabla^2 C_1^{40} \\ & - \nabla f_1^{40} D_1^{44} \nabla C_1^{44} - f_1^{40} D_1^{44} \nabla^2 C_1^{44} \\ & + \nabla f_1^{40} D_{11}^{40} \nabla C_1 + f_1^{40} D_{11}^{40} \nabla^2 C_1 \\ & + \nabla f_1^{40} D_{12}^{40} \nabla C_2 + f_1^{40} D_{12}^{40} \nabla^2 C_2 \end{aligned} \tag{16a}$$

$$\begin{aligned} \frac{\partial C_1^{44}}{\partial t} = {} & D_1^{44} \nabla^2 C_1^{44} - \nabla f_1^{44} D_1^{44} \nabla C_1^{44} - f_1^{44} D_1^{44} \nabla^2 C_1^{44} \\ & - \nabla f_1^{44} D_1^{40} \nabla C_1^{40} - f_1^{44} D_1^{40} \nabla^2 C_1^{40} \\ & + \nabla f_1^{44} D_{11}^{44} \nabla C_1 + f_1^{44} D_{11}^{44} \nabla^2 C_1 \\ & + \nabla f_1^{44} D_{12}^{44} \nabla C_2 + f_1^{44} D_{12}^{44} \nabla^2 C_2 \end{aligned} \tag{16b}$$

$$\frac{\partial C_2}{\partial t} = D_{21} \nabla^2 C_1 + D_{22} \nabla^2 C_2. \tag{16c}$$

Since chemical diffusion coefficients for CaO are dependent on mobility, there are up to three parameters that could describe the mass dependence on diffusion coefficients: β_1, β_{11} and β_{12} (Eq. (8)). Before presenting model isotope ratio profiles, it is important to assess how one should treat these β factors; for example, how do differences in isotopic mobilities translate into differences in isotope-specific diffusion matrix elements? Should these β factors be treated independent of one another? Or, can β_{11} and β_{12} be written in terms of a single parameter β_1?

5.3.1. Relationship between mobility and chemical diffusion coefficients

We analyze in Appendix A.2 how varying the self diffusivity of Ca may affect the diagonal and off-diagonal diffusion matrix elements of CaO. To summarize, there are at least two distinct approaches, one in which only the diagonal element is mass dependent, hereafter referred to as the Common Velocity (CV) Model, and one in which both the diagonal and off-diagonal elements are mass dependent, hereafter referred to as the Common Force (CF) Model. The CV model assumes that each component has the same velocity relative to its random walk velocity arising from self diffusion regardless of differences in the interaction forces between them. The CF model, on the other hand, assumes that differences between particles are manifested in how they respond to common interaction forces (cf. Liang, 1994). The two sets of curves in Fig. 3e and h show the Δ^{44}Ca profiles for A–B and D–E resulting from the CV and CF Models. For the CV Model, the β factors differ between experiments A–B and D–E; a larger β_i is required to reproduce the larger magnitude of isotopic fractionations in experiment A–B. This compositional/directional dependence required by the CV Model, in some sense, defeats the original purpose of the multicomponent diffusion formulation. The CF Model, on the other hand, has the property that a single set of β factors can fit the profiles for the two orthogonal directions of diffusion in composition space.

6. DISCUSSION

6.1. Why does CaO diffuse faster in A–B than D–E?

During multicomponent diffusion, a net flux of a major component must be counter-balanced by a flux of other components in the liquid. The implication of the no net volume flux constraint is that fast diffusing components can enhance the diffusive flux of slower diffusing components and vice versa. This inference is compatible with the information contained in the diffusivity matrix. In couple A–B, the gradients in CaO and Na_2O oppose one another but the off-diagonal term $D_{CaO-Na2O}$ is negative. Hence the term $D_{CaO-Na_2O}\nabla C_{Na_2O}$ reinforces the flux of CaO down its concentration gradient. In couple D–E, the opposite is true. Gradients in CaO and SiO_2 oppose one another but the off-diagonal term $D_{CaO-SiO_2}$ is positive. Since $|D_{CaO-CaO}\nabla C_{CaO}| > |D_{CaO-SiO_2}\nabla C_{SiO_2}|$, the net flux of CaO is in the direction of its own concentration gradient but is somewhat inhibited owing to the contribution of the $D_{CaO-SiO_2}\nabla C_{SiO_2}$ term.

The top panels of Fig. 4 quantify the sensitivity of EBDCs to the direction of diffusion in composition space. In experiment A–B, $D^E_{CaO} \approx 140 \times 10^{-12}$ m^2/s, whereas in D–E, $D^E_{CaO} \approx 40 \times 10^{-12}$ m^2/s. The fact that these two values bracket the self diffusivity of Ca, which is about 80×10^{-12} m^2/s, provides a clear indication that rates of isotope homogenization are not necessarily faster than rates of chemical homogenization, in contrast to previous proposals (Baker, 1989; Lesher, 1990, 1994).

6.2. Self diffusion is not necessarily faster than chemical diffusion

The view that isotopes equilibrate faster than the parent elements in an inhomogeneous liquid seems to arise in part from the intuition that isotopes equilibrate at a rate that depends on the self diffusion coefficient while the parent element equilibrates at a rate that depends on the chemical diffusion coefficient(s). Note that if this were true, there would be cases where the isotopes would equilibrate more slowly such as when self diffusion is slower than chemical diffusion as pointed out in Section 6.1. The idea that isotopes will equilibrate at a rate given by the self diffusivity, while the parent element will equilibrate at a rate given by the chemical diffusion coefficients is most easily shown to be not generally true in situations where self diffusion is much faster than chemical diffusion. Consider for example experiment RB2 by Richter et al. (2003) involving the interdiffusion of molten rhyolite and basalt. All the major elements in this experiment homogenized at the same rate as the slowly diffusing SiO_2 component. Isotope fractionation of Ca was observed as being restricted to the diffusion boundary layer of CaO. Given that the rate of self diffusion of Ca is much larger than its EBDC in the rhyolite-basalt diffusion couple, if the isotopes were homogenizing at a rate given by the self diffusion coefficient, then the isotopic fractionations would be spread well beyond the chemical diffusion boundary layer, which was clearly not the case. This same result of the isotopic fractionation being restricted to the parent element diffusion boundary layer can be seen in the experimental results shown in Figs. 3 and 4. Yet another demonstration that isotopic homogenization is not generally faster than homogenization of the parent element was given by Richter et al. (2014) who showed that the isotopic fractionation of lithium diffused into augite persisted almost ten times longer than the time required for the lithium concentration to become uniform.

6.3. Why are isotope effects greater in A–B than D–E?

The isotopic results from A–B and D–E suggest that for a given temperature, pressure, and bulk composition, faster chemical diffusion promotes larger diffusive isotopic fractionations. This agrees with what has been observed in diffusion experiments using natural silicate liquids as well as simplified silicate liquids, albeit for different reasons (Richter et al., 2003, 2009; Watkins et al., 2009, 2011). The conclusion from previous studies (cf. Watkins et al., 2011; Goel et al., 2012) is that the degree of mass discrimination between isotopes relates directly to the bonding of

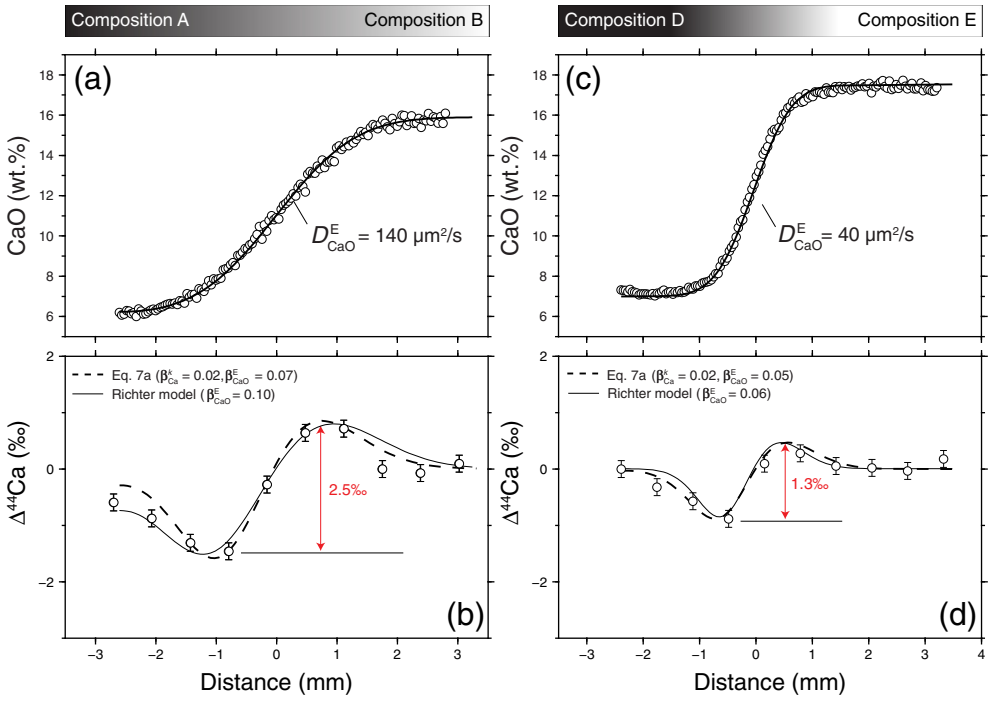

Fig. 4. Application of effective binary diffusion models to experimental results. Solid lines are model profiles produced using the EBD models with a mass dependence on diffusivity parameters. The estimated confidence interval on the β parameters is about ± 0.01. In the Richter model, the isotopic fluxes are treated independent of one another and there is no self diffusion term. In Eq. (7a) there is a mass dependence on self diffusivity as well as the EBDC. The β factors deduced from either of these two EBD models vary with the direction of diffusion in composition space, and are therefore non-generalizable for a given bulk composition.

the elements to the alumino-silicate melt structure, such that the fractionation behavior of the cations varies with liquid composition as melt structure changes. In basaltic liquids, CaO is strongly bound to the Al–Si framework and consequently diffuses at about the same rate as SiO_2 ($D^E_{CaO}/D^E_{SiO_2} \approx 1$) and has relatively small mass discrimination. In high silica liquids calcium is not strongly bound to the Al–Si framework, diffuses much faster than SiO_2 ($D^E_{CaO}/D^E_{SiO_2} \gg 1$) and has relatively large mass discrimination. The physical interpretation is that in high-Si liquids Ca apparently diffuses more or less as an ion through the quasi-stationary Al–Si matrix; hence its mass discrimination ($\beta^E_i = 0.18$) approaches the kinetic-theory prediction for a dilute, monatomic gas: $\beta^E_i = 0.5$ (i.e., $D \propto m^{-0.5}$). In mafic liquids, however, diffusion of Ca involves the cooperative motion of a larger number of atoms (cf. Goel et al., 2012), and the mass discrimination is reduced to ≈10% of that expected for $m^{1/2}$ dependence ($\beta^E_i \approx 0.03$).

In this study, the mass discrimination that accompanies diffusion of an oxide component that is present in major quantities clearly depends on the cooperative motions of other components in the liquid. The exact nature of oxide-oxide coupling is complicated, even with complete knowledge of the full diffusion matrix (Liang et al., 1996). Nevertheless, several key insights into how each component affects the isotopic fractionations of Ca can be obtained by examining the elements of the diffusion matrix for different choices of dependent component. If the D^k_{ij}'s and β_{ij}'s are known for one choice of dependent component, they can be recast for different choices of dependent component using the following relations based on Eq. (6)a–d in Liang et al. (1996):

$$\frac{{}^2D^{44}_{11}}{{}^2D^{40}_{11}} = \frac{{}^3D^{44}_{11} - {}^3D^{44}_{12}}{{}^3D^{40}_{11} - {}^3D^{44}_{12}} = \left(\frac{m_{40}}{m_{44}}\right)^{{}^2\beta_{11}} \tag{17a}$$

$$\frac{{}^2D^{44}_{13}}{{}^2D^{40}_{13}} = \frac{-{}^3D^{44}_{12}}{-{}^3D^{40}_{12}} = \left(\frac{m_{40}}{m_{44}}\right)^{{}^2\beta_{13}} \tag{17b}$$

Substituting Eqs. (17a) and (17b) into Eq. (8b), we arrive at the following relationships between β's for different components in a three-component system:

$${}^2\beta_{11} = \frac{\ln\left[\frac{{}^3D^{40}_{11}\left(\frac{40}{44}\right)^{{}^3\beta_{11}} - {}^3D^{40}_{12}\left(\frac{40}{44}\right)^{{}^3\beta_{12}}}{{}^3D^{40}_{11} - {}^3D^{40}_{12}}\right]}{\ln\left(m_{40}/m_{44}\right)} \tag{18a}$$

and

$${}^2\beta_{13} = {}^3\beta_{12}. \tag{18b}$$

An interesting property of a ternary system is that the off-diagonal beta factors share the same magnitude and sign regardless of the choice of dependent component. This is in contrast to the off-diagonal elements of the diffusion matrix, which share the same magnitude but are opposite in sign (Eq. (14) versus Eq. (15)). The implication is that for any CaO-bearing three component system, one of the components (Na_2O in this case) will enhance the diffusive flux of CaO, with preferential enhancement of the flux of

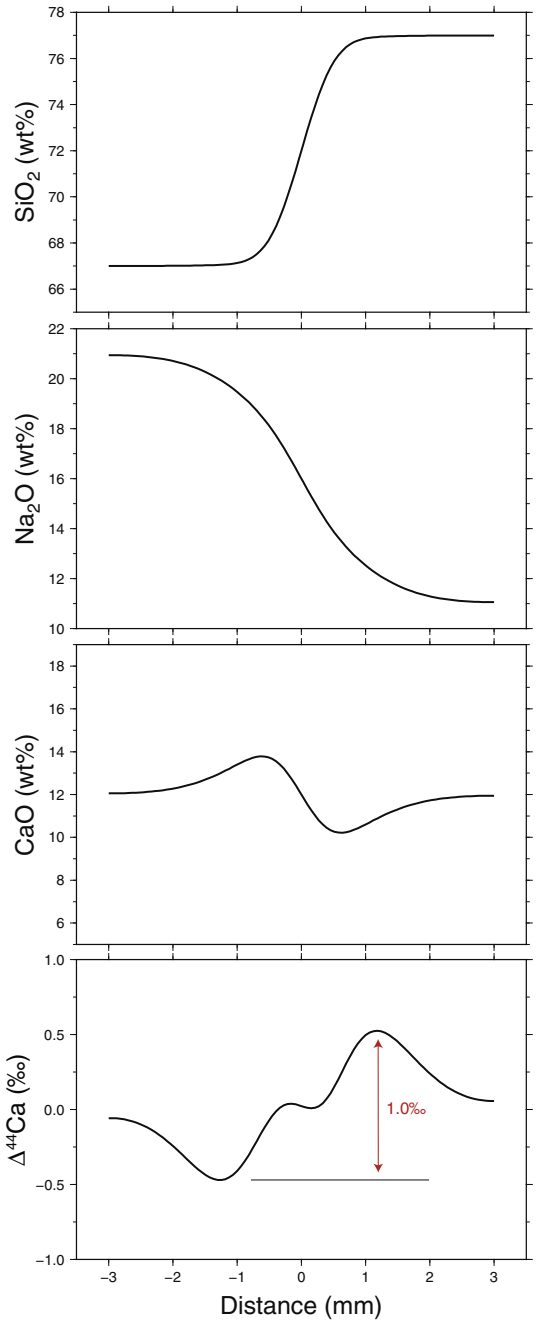

Fig. 5. Expected Ca isotopic fractionations due to diffusive coupling in the system $16Na_2O{\cdot}12CaO{\cdot}72SiO_2$ based on the known diffusion matrix and assuming the Common Force (CF) model parameters in Fig. 3. The hypothetical diffusion couple is oriented such that there is no initial CaO concentration gradient. The CaO profile indicates a net flux of CaO from right to left, leading to light Ca enrichment on the left-hand side of the couple. These calculations suggest that relatively large diffusive isotope effects can arise even in the absence of a large concentration gradient in the parent element.

^{40}Ca relative to ^{44}Ca in the direction that CaO is diffusing. The other component (SiO_2 in this case) will drag CaO in the direction opposite of the CaO concentration gradient, preferentially dragging ^{40}Ca relative to ^{44}Ca in the direction opposite the CaO gradient. If the CF Model approach is correct, the implication is that diffusion of CaO against the component with a negative off-diagonal term should, in general, tend to maximize the magnitude of diffusive isotopic fractionations. *A direct consequence is that, for a given set of β factors, major element diffusive isotope effects should be largest for the direction of diffusion in which the diffusive flux is greatest.*

The above generalizations lead to interesting predictions for isotopic fractionations due to diffusive coupling. Consider the case where SiO_2 and Na_2O counter diffuse in the presence of a small CaO gradient (Fig. 5). As SiO_2 diffuses from right to left, it preferentially enhances the diffusive flux of ^{40}Ca relative to ^{44}Ca from right to left. As Na_2O diffuses from left to right, it also preferentially enhances the diffusive flux of ^{40}Ca relative to ^{44}Ca from right to left. The net result is a superposition of isotopic fractionations that are quite large (~1‰) despite the lack of an initial CaO concentration gradient. An attempt was made to perform this experiment, but the experiment was unsuccessful due to incomplete melting of the SiO_2-rich side of the couple at 1250 °C. Nevertheless, it appears that diffusive coupling is capable of generating relatively large (>1‰) isotopic fractionations even when the initial concentration contrast for the diffusing element is small, as was originally suggested by Watkins et al. (2009).

6.4. Isotope fractionation by effective binary diffusion

For the isotope fractionation by diffusion problem, it has been customary to treat each isotope as an independent chemical species, diffusing in response to its own concentration gradient (Richter et al., 1999, 2003, 2009; Chopra et al., 2012). The advantage of this approach is that only one β_i^E parameter is needed to model the isotopic fractionations but a disadvantage is that it neglects any isotopic exchange during the diffusion of isotopes. For couples A-B and D-E, both the Richter model and the new EBD model (Eq. (7a), which involves a mass dependence on self diffusivity as well as the EBDC) can produce profiles that are in excellent agreement with the data (Fig. 4). For the Eq. (7a)a profiles we assume $\beta_{Ca}^k = 0.02$ for consistency with the CF model results in Fig. 3. The main conclusion that can be drawn from Fig. 4 is that regardless of which model is used, it is clear that for effective binary diffusion of major elements, the inferred β_i^E's, like the EBDCs, are non-generalizable in that they vary depending on the direction of diffusion in composition space.

Although the Richter et al. (2003) approach has the major advantage of involving only one free parameter, in some cases it leads to model isotope ratio profiles that do not exactly match the spatial variations in diffusive isotopic fractionations (Richter et al., 2003, 2009; Watkins et al., 2009; Chopra et al., 2012), and some of the misfit may be due to neglecting the role of self diffusion. The self diffusion terms in Eq. (7a) contribute to the modeled isotopic fractionations in two ways. First, an increase in the self diffusivity D_i^k relative to the EBDC reduces the isotopic fractionations and broadens the low Δ^{44}Ca troughs. This

behavior was pointed out by Watkins et al. (2011), who analyzed diffusive isotopic fractionations of Ca and Mg in simplified, albite-rich liquids. In their analysis, Watkins et al. (2011) showed how accounting for self diffusion superimposed on chemical diffusion could better fit the data from experiments where it was clear that diffusive isotope effects extended noticeably beyond the CaO diffusion profiles. The second influence of self diffusion is that, according to the behavior of Eq. (7a), it does not act solely to homogenize the isotope ratios, but rather, its mass dependence enhances the diffusive isotopic fractionations. That is, the isotope ratio profiles are sensitive to D_i^k, D_i^E, β_i and β_i^E. Hence, although Eq. (7a) may be a more accurate representation of the isotope fluxes in space and time than the Richter model, its accuracy comes at the expense of two additional parameters (D_i^k and β_i) while still being subject to the limitations of EBD models in general as described in Section 2.2.

7. SUMMARY AND FURTHER DISCUSSION

Diffusion couple experiments on simplified systems provide valuable clues about the nature of mass discrimination during chemical transport in geological systems. Previous studies on Ca and Mg diffusion in albite-rich liquids showed that mass discrimination during diffusion varies with liquid composition, and also varies between cations for a given liquid composition (Watkins et al., 2009, 2011). Furthermore, faster diffusing cations such as Li, tend to exhibit larger mass discrimination (Richter et al., 2003;Watkins et al., 2011). The key observation from the experiments in this study is that the rate of diffusion, as well as the isotopic fractionations that arise during diffusive transport in molten silicates, varies depending on how a diffusion couple is oriented in composition space. In one experiment (A–B), CaO and Na_2O counter-diffuse rapidly in the presence of a small SiO_2 gradient and the Ca isotope fractionations are relatively large (~2.5‰). In the other experiment (D–E), CaO and SiO_2 counter-diffuse more slowly in a small Na_2O gradient and the Ca isotope fractionations are reduced (~1.3‰). Hence for a given liquid composition, the orientation of the diffusion couple in composition space that promotes faster diffusion seems to also promote larger diffusive isotopic fractionations.

Observations such as these help guide the theory of isotope diffusion in complex liquids. We presented a new formulation for isotope diffusion that takes into account both self diffusion and chemical diffusion. Kinetic theory predicts a mass dependence on the self diffusivity D_i^k, which represents a cation's mobility, but no prior study to our knowledge has specifically addressed how a mass dependence on mobility translates into a mass dependence on chemical diffusion coefficients. We discussed two classes of models that relate self diffusivities to elements of the diffusion matrix: the common-velocity (CV) models predict a mass dependence on diagonal terms alone whereas the common-force (CF) models predict a mass dependence on diagonal as well as off-diagonal terms. The CF models correctly reproduce the observed behavior; i.e., a single set of β's can account for different degrees of isotopic fractionation for diffusion along two roughly orthogonal directions in composition space. This result is particularly intriguing in light of the fact that Liang et al. (1997) found that the CF models fit the observed diffusion profiles and diffusion matrices better than other empirical models in the $CaO–Al_2O_3–SiO_2$ (CAS) system. The CF models also predict that (a) diffusive isotope effects should be maximized for the direction of diffusion that maximizes the diffusive flux and (b) diffusive coupling may give rise to relatively large isotopic fractionations even in the absence of a large concentration gradient in the diffusing element. This latter prediction is consistent with previous observations in natural volcanic liquids (Watkins et al., 2009).

The equations presented herein argue against the idea that self diffusion and chemical diffusion are decoupled from one another (Lesher, 1990, 1994). The experimental data further show that self diffusion can be either faster than or slower than chemical diffusion, depending on the direction of diffusion in composition space. The new formulations for isotope diffusion can be tested with further experimentation and should aid in the identification and interpretation of isotopic variations in nature. Moving forward, it will be informative to investigate isotopic diffusion in a $CaO–Al_2O_3–SiO_2$ liquid where the self diffusivities and thermodynamic relationships are known (Liang et al., 1996, 1997). Additional information could be gained by investigating diffusive isotopic fractionations for multiple elements, e.g., in a $CaO–MgO–Al_2O_3–SiO_2$ liquid in which isotopic variations in both Ca and Mg can be measured. Although the theory of diffusive mass transport is relatively mature, there are still key aspects of isotope diffusion that are not well understood.

ACKNOWLEDGMENTS

Ben Jacobsen contributed the SIMS measurements shown in Fig. 2. This research was supported by National Science Foundation Grants EAR-1050000 to D.J.D. and EAR-1220076 to Y.L., and U.S. Department of Energy Grant DE-FG02-01ER15254 to F.M.R.

APPENDIX A

A.1. Alternative formulation for the isotopic flux

The expression for the isotopic flux (Eq. (2)) differs slightly from an expression that has been used in previous studies of isotope diffusion (e.g., Richter et al., 1999; Watkins et al., 2011). The expression used by Richter et al. (1999) was arrived at by considering deviations in self diffusivity (Liang, 1994):

$$J_i^k = -D_i^k \nabla C_i^k + \sum_{m=1}^{M} f_i^k (D_i^m - D_i^k + D_i^k) \nabla C_i^m - \sum_{j=1}^{n-1} f_i^k D_{ij}^k \nabla C_j. \quad (A.1)$$

Since $C_i = C_i^1 + C_i^2 + \cdots + C_i^M$, Eq. (A.1) can also be written as

$$J_i^k = \underbrace{-D_i^k \nabla C_i^k + \sum_{j=1}^{n-1} f_i^k (D_{ij}^k - D_i^k \delta_{ij}) \nabla C_j}_{\text{Richteretal.(1999)}} + \underbrace{\sum_{m=1}^{M} f_i^k (D_i^m - D_i^k) \nabla C_i^m}_{\text{negligible?}}. \quad (A.2)$$

The first two terms in Eq. (A.2) are identical to the Richter et al. (1999) flux equation except that here the D_{ij}'s are written with a superscript k to denote that they are isotope-specific. The third term was previously neglected because diffusivity differences among the isotopes of i are known to be very small (i.e., second order terms) and therefore negligible in many applications. However, these small terms affect the inferred β factors in studies of isotope fractionation by diffusion even though the first two terms on the RHS of Eq. (A.2) are relatively large. To illustrate this point, Fig. A.1 compares the result one would obtain using all three terms of Eq. (A.2) versus the result obtained by Richter et al. (1999) using only the first two terms. Although the fits are nearly identical for both approaches, the inferred β factor is about 3 times greater when the third term of Eq. (A.2) is neglected. Hence, although diffusivity differences among isotopes are small they cannot be neglected in the special case of stable isotope fractionation by diffusion.

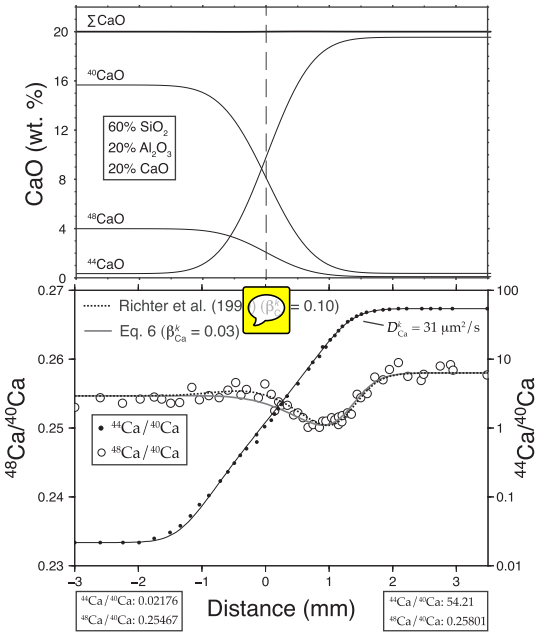

Fig. A.1. Self diffusion experiment from Richter et al. (1999) designed to measure the self diffusivity of Ca and its mass dependence in molten $CaO–Al_2O_3–SiO_2$ at 1500 °C and 1 GPa. The initial composition of each half of the diffusion couple is shown in the boxes at the bottom of the figure. The self diffusion coefficient D_i^k is determined from the fit to the $^{44}Ca/^{40}Ca$ profile and its mass dependence is inferred from the fit to the $^{48}Ca/^{40}Ca$ profile. The curves represent model results using two different expressions for the isotopic flux. Although the fits are nearly identical, the inferred β factors differ significantly depending on which formulation is used, thus demonstrating that the third term in Eq. (A.1) is non-negligible.

A.2. Relationship between mobility and chemical diffusion coefficients

Diffusive fluxes are related to concentration gradients by

$$J_i = -\sum_{k=1}^{n-1} D_{ik} \nabla C_k. \quad (A.3)$$

For self diffusion, if we treat the isotopes as "independent" components and assume that (a) the partial molar volumes of isotopes are equal and (b) diffusive mixing of isotopes is thermodynamically ideal, then we arrive at a general expression for self diffusion (Eq. (6)) (Liang et al., 1997). The expression for self diffusion is added to the expression for chemical diffusion (Eq. (4)) using the principle of superposition for linear partial differential equations to arrive at the flux expression for the combined chemical and self diffusion equation (Eq. (2)).

The diffusion matrix [**D**] can be written as a product of a thermodynamic matrix [**G**] and a kinetic matrix [$\mathcal{L}$] (Onsager, 1945):

$$[\mathbf{D}] = [\mathcal{L}] \cdot [\mathbf{G}] \quad (A.4)$$

or

$$D_{ik} = \sum_{j=1}^{N-1} \mathcal{L}_{ij} G_{jk} \quad (A.5)$$

The elements of the thermodynamic matrix [**G**] are functions of model-independent activity-composition relations and can be written as (Liang et al., 1997):

$$G_{jk} = C_j \left(\frac{\partial \ln a_j}{\partial C_k} - \frac{V_k}{V_n} \frac{\partial \ln a_j}{\partial C_n} \right), \quad (A.6)$$

where component n is the dependent component; a is activity; C_i and V_i are the molar concentration and partial molar volume of component i. In many systems, including the $16Na_2O{\cdot}12CaO{\cdot}72SiO_2$ system, the activity-composition relations are not known. In an ideal liquid where $a_j = C_j$ and in the special case where partial molar volumes of components are equal, the thermodynamic matrix reduces to the identity matrix. For simplicity, we adopt this ideal solution model and assume further that the activities and partial molar volumes of isotopically-substituted oxides are equal.

The diffusion matrix elements are related to self diffusivities through the kinetic [$\mathcal{L}$] matrix. A general expression for building the model-dependent [$\mathcal{L}$] matrix is (Liang, 1994, 2010; Liang et al., 1997):

$$\mathcal{L}_{ij} = D_j \delta_{ij} + C_i \left[(V_n D_n - V_j D_j) A_i + (p_n z_n D_n - p_j z_j D_j) B_i \right], \quad (A.7)$$

where component n is the dependent component; D_j and z_j are the self diffusivity and charge number of cation j, respectively; C_i and V_j are the molar concentration and partial molar volume of components i and j, respectively; p_j is the stoichiometric coefficient of the cation in oxide component j (e.g., $p = 2$ for Na_2O); and A_i and B_i are scaling factors (cf. Liang, 2010). For example, $(A_i, B_i) = (1, 0), (1, \tau_i), (\phi_i, 0)$, and (Ω_i, Φ_i), for the molecular

common-velocity model, ionic common-velocity model, molecular common-force model, and ionic common-force model, respectively. The full expressions for the scaling factors are (Liang, 1994; Liang et al., 1997):

$$\tau_i = \frac{\sum_{j=1}^{n}(\delta_{ij} - C_{io}V_{jo})C_{jo}z_jD_j}{\sum_{j=0}^{n}C_jz_j^2D_j}, \quad (A.8)$$

$$\phi_i = \frac{V_iD_i}{\sum_{k=1}^{n}C_kV_k^2D_k}, \quad (A.9)$$

$$\Omega_i = \frac{M_i(z_iW_{22} - V_{io}/p_iW_{21})}{W_{11}W_{22} - W_{12}W_{21}}, \quad (A.10)$$

and

$$\Phi_i = \frac{C_{io}M_i(V_i/p_iW_{11} - z_iW_{12})}{W_{11}W_{22} - W_{12}W_{21}}, \quad (A.11)$$

where

$$W_{11} = \sum_{i=1}^{n}C_{io}V_{io}z_iM_i, \quad W_{12} = \sum_{i=1}^{n}\frac{C_{io}V_{io}^2M_i}{p_i}, \quad (A.12)$$
$$W_{21} = \sum_{i=0}^{n}C_iz_i^2M_i, \quad W_{22} = W_{11}.$$

In the above equations, the subscript '*io*' refers to the *i*-bearing oxide component. The only measurable quantities one needs in order to calculate the diffusion matrix elements are (1) the self diffusivities and (2) the partial molar volumes. Isotope-specific elements of the diffusion matrix are calculated by substituting the isotope-specific mobilities into the above expressions. The ratio of isotopic diffusion coefficients is then expressed in terms of β factors using Eq. (8b). Table A.1 shows the values of β_{11} and β_{12} calculated from $\beta_1 = 0.1$, partial molar volumes from Lange (1997) and using placeholder values for the self diffusivities of Na and Si. Using different values of the self diffusivities would not affect the following conclusions: (1) $\beta_{i=j} \approx \beta_i$ for all four models, (2) $\beta_{i\neq j} \approx 0$ for the common-velocity models, and (3) $\beta_{i\neq j} \approx \beta_i$ for the common-force models. Hence there are at least two distinct approaches to investigate, one in which only the diagonal element is mass dependent, hereafter referred to as CV Model, and one in which both the diagonal and off-diagonal elements are mass dependent, hereafter referred to as CF Model.

Table A.1
Comparison between four different empirical models that relate how a mass dependence on the self diffusivity β_i translates into a mass dependence on diffusion matrix elements β_{ij}. For these calculations we used partial molar volumes from Lange (1997) and the following self diffusivities: $D^k_{Ca} = 80 \times 10^{-12}$ m^2/s, $D^k_{Na} = 140 \times 10^{-12}$ m^2/s, and $D^k_{Si} = 30 \times 10^{-12}$ m^2/s.

Model	(A_i, B_i)	β_1	β_{11}	β_{12}
Molecular common velocity	(1,0)	0.1	0.093	0
Ionic common velocity	$(1,\tau_i)$	0.1	0.093	0.019
Molecular common force	$(\phi_i,0)$	0.1	0.101	0.093
Ionic common force	(Ω_i, Φ_i)	0.1	0.092	0.092

REFERENCES

Baker D. R. (1989) Tracer versus trace element diffusion: diffusional decoupling of Sr concentration from Sr isotope composition. *Geochim. Cosmochim. Acta* **53**(11), 3015–3023.

Chakraborty S., Dingwell D. and Rubie D. (1995) Multicomponent diffusion in ternary silicate melts in the system K_2O–Al_2O_3–SiO_2 II: mechanisms, systematics, and geological applications. *Geochim. Cosmochim. Acta* **59**, 265–277.

Chopra R., Richter F., Bruce Watson E. and Scullard C. (2012) Magnesium isotope fractionation by chemical diffusion in natural settings and in laboratory analogues. *Geochim. Cosmochim. Acta*.

Cooper A. (1968) The use and limitations of the concept of an effective binary diffusion coefficient for multicomponent diffusion. *Mass Transport Oxides* **296**, 79–84.

de Groot S. R. and Mazur P. (1963) *Non-equilibrium Thermodynamics*. North-Holland.

Goel G., Zhang L., Lacks D. and Van Orman J. (2012) Isotope fractionation by diffusion in silicate melts: insights from molecular dynamics simulations. *Geochim. Cosmochim. Acta*.

Kress V. and Ghiorso M. (1993) Multicomponent diffusion in MgO–Al_2O_3–SiO_2 and CaO–MgO–Al_2O_3–SiO_2 melts. *Geochim. Cosmochim. Acta* **57**(18), 4453–4466.

Lange R. A. (1997) A revised model for the density and thermal expansivity of K_2O–Na_2O–CaO–MgO–Al_2O_3–SiO_2 liquids from 700 to 1900 K: extension to crustal magmatic temperatures. *Contrib. Mineral. Petrol.* **130**(1), 1–11.

Lesher C. (1990) Decoupling of chemical and isotopic exchange during magma mixing.

Lesher C. (1994) Kinetics of Sr and Nd exchange in silicate liquids: theory, experiments, and applications to uphill diffusion, isotopic equilibration, and irreversible mixing of magmas. *J. Geophys. Res.* **99**(B5), 9585–9604.

Liang Y. (1994) Models and experiments for multicomponent diffusion in molten silicates. Ph. D. thesis, University of Chicago.

Liang Y. (2010) Multicomponent diffusion in molten silicates: theory, experiments, and geological applications. *Rev. Mineral. Geochem.* **72**(1), 409–446.

Liang Y., Richter F. M. and Chamberlin L. (1997) Diffusion in silicate melts III: empirical models for multicomponent diffusion. *Geochim. Cosmochim. Acta* **61**(24), 5295–5312.

Liang Y., Richter F. M. and Watson E. B. (1996) Diffusion in silicate melts II: multicomponent diffusion in CaO–Al_2O_3–SiO_2 at 1500 °C and 1 GPa. *Geochim. Cosmochim. Acta* **60**, 5021–5035.

Onsager L. (1945) Theories and problems of liquid diffusion. *Ann. NY Acad. Sci.* **46**(5), 241–265.

Richter F., Davis A., DePaolo D. and Watson E. (2003) Isotope fractionation by chemical diffusion between molten basalt and rhyolite. *Geochim. Cosmochim. Acta* **67**(20), 3905–3923.

Richter F., Liang Y. and Davis A. (1999) Isotope fractionation by diffusion in molten oxides. *Geochim. Cosmochim. Acta* **63**(18), 2853–2861.

Richter F., Liang Y. and Minarik W. (1998) Multicomponent diffusion and convection in molten MgO–Al_2O_3–SiO_2. *Geochim. Cosmochim. Acta* **62**(11), 1985–1991.

Richter F., Watson E., Mendybaev R., Dauphas N., Georg B., Watkins J. and Valley J. (2009) Isotopic fractionation of the major elements of molten basalt by chemical and thermal diffusion. *Geochim. Cosmochim. Acta* **73**, 4250–4263.

Richter F., Watson B., Chaussidon M., Mendybaev R. and Ruscitto D. (2014) Lithium isotope fractionation by diffusion in minerals. Part 1: Pyroxenes. *Geochim. Cosmochim. Acta* **126**, 352–370.

Roskosz M., Luais B., Watson H., Toplis M., Alexander C. and Mysen B. (2006) Experimental quantification of the fractionation of Fe isotopes during metal segregation from a silicate melt. *Earth Planet. Sci. Lett.* **248**(3), 851–867.

Sugawara H., Nagata K. and Goto K. (1977) Interdiffusivities matrix of $CaO–Ai_2O_3–SiO_2$ melt at 1723 K to 1823 K. *Metall. Mater. Trans. B* **8**(4), 605–612.

Trial A. and Spera F. (1994) Measuring the multicomponent diffusion matrix: experimental design and data analysis for silicate melts. *Geochim. Cosmochim. Acta* **58**(18), 3769–3783.

Wakabayashi H. and Oishi Y. (1978) Liquid-state diffusion of $Na_2O–CaO–SiO_2$ system. *J. Chem. Phys.* **68**, 2046.

Watkins J., DePaolo D., Huber C. and Ryerson F. (2009) Liquid composition-dependence of calcium isotope fractionation during diffusion in molten silicates. *Geochim. Cosmochim. Acta* **73**(24), 7341–7359.

Watkins J., DePaolo D., Ryerson F. and Peterson B. (2011) Influence of liquid structure on diffusive isotope separation in molten silicates and aqueous solutions. *Geochim. Cosmochim. Acta* **75**(11), 3103–3118.

Associate editor: Dimitri A. Papanastassiou